Published in Applied Optics 31, issue 26, 5706-5711, 1992
which should be used for any reference to this work

Optimized kinoform structures for highly efficient fan-out elements

D. Prongué, H. P. Herzig, R. Dändliker, and M. T. Gale

We discuss the realization of highly efficient fan-out elements. Laser-beam writing lithography is available now for fabricating smooth surface relief microstructures. We develop several methods for optimizing microstructure profiles. Only a small number of parameters in the object plane are necessary for determining the kinoform. This simplifies the calculation of $M \times N$ arrays also for large M and N. Experimental results for a 9-beam fan-out element are presented.

Key words: Fan-out, kinoform, phase grating, computer-generated hologram, holographic optical element.

I. Introduction

Phase elements that generate arrays of light spots are key components in many optical processing systems. Space-invariant fan-out elements split a laser beam into N quasi-plane waves, which are focused by a Fourier lens, as shown in Fig. 1.

Different types of fan-out elements have been investigated in the past. Binary phase holograms, such as Dammann gratings, are well known. Their fabrication involves microlithographic techniques that are well mastered and widely available. However, these elements are usually limited by their efficiency. In order to increase the diffraction efficiency, recent efforts have concentrated on multilevel phase structures, such as quaternary phase elements[1] or off-axis multilevel phase elements.[2] Their fabrication also involves microlithography, but with the drawback that the number of masks increases with the number of phase levels. Thus precise alignment must be performed during each process.

In our approach we optimize a nonquantized phase transfer function for an on-axis fan-out element and we implement this phase function as a smooth surface relief grating. This process became possible with the laser-beam writing system developed at the Paul Scherrer Institute, Zürich.[3,4] This method has the advantage of being able to generate smooth surfaces, which can have maximum diffraction efficiency, and to draw the structure in one single step, which avoids errors that are due to successive alignments. On the other hand the control of the modulation depth can be difficult, depending on the knowledge and stability of the photoresist and development parameters.

We have developed a two-step method to optimize the transfer function of a fan-out element.[5,6] The optimization criteria are the efficiency and the uniformity of the outgoing beams. The optimization parameters are the amplitudes and phases of an array of recorded virtual light sources. These sources are called virtual because they are used only to describe the construction of the fan-out element, but they are not physically used to record the fan-out element. The small number of free parameters and the nonquantized phase function in the hologram plane leads to fast optimization procedures.

We applied the optimization method to a nine-beam fan-out and we recorded its transfer function into photoresist. The resulting element is an on-axis surface relief phase hologram.

II. Kinoform Optimization

The goal of our fan-out element is to focus a laser beam onto a regular array of equally intense light spots. The desired field distribution in the object plane (Fig. 1) is then given by

$$U(x, y) = \sum_{m=1}^{N} A_m \exp(i\phi_m)\delta(x - x_m, y), \tag{1}$$

where A_m is the amplitude, ϕ_m is the phase, and x_m is the position of the mth spot of a one-dimensional array. The phases ϕ_m are free parameters.

M. T. Gale is with the Paul Scherrer Institute, Badenerstrasse 569, CH-8048 Zürich, Switzerland. The other authors are with the Institute of Microtechnology, University of Neuchâtel, CH-2000 Neuchâtel, Switzerland.

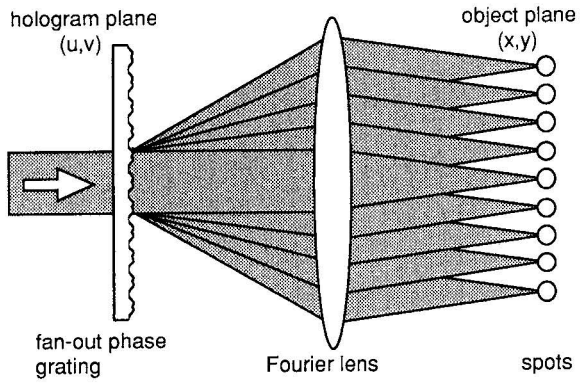

Fig. 1. Readout of the fan-out element.

The field distribution $\hat{U}(u, v)$ in the hologram plane is related to the field $U(x, y)$ by a Fourier transform:

$$\hat{U}(u, \mathrm{v}) = \int_{-\infty}^{\infty} U(x, y)\exp[2\pi i(xu + yv)]\mathrm{d}x\mathrm{d}y = \sum_{m=1}^{N} A_m \exp(i\phi_m)\exp(2\pi i x_m u). \quad (2)$$

The field $\hat{U}(u, v)$ written in terms of magnitude and phase is

$$\hat{U}(u, v) = |\hat{U}(u, v)|\exp[i\psi(u, v)], \quad (3)$$

where $\psi(u, v) = \arg\{\hat{U}\}$. For the irradiance distribution $I(u, v)$ in the hologram plane we obtain

$$I(u, v) = |\hat{U}(u, v)|^2 = \sum_{m=1}^{N} A_m{}^2 + 2\sum_{m<n}^{N} A_m A_n \cos(\Omega_{mn}), \quad (4)$$

where the arguments Ω_{mn} stand for

$$\Omega_{mn} = 2\pi u(x_m - x_n) + \phi_m - \phi_n. \quad (5)$$

For a constant distance s between the spots the arguments Ω_{mn} in Eq. (5) become

$$\Omega_{mn} = 2\pi u(m - n)s + \phi_m - \phi_n. \quad (6)$$

The first term on the right side of Eq. (4) is constant and is equal to the mean object irradiance,

$$\langle I\rangle = \langle|\hat{U}|^2\rangle = \sum_{m=1}^{N} A_m{}^2. \quad (7)$$

The second term describes the irradiance variations, or intermodulations, in the hologram plane.

In order to perfectly reproduce the desired object $U(x, y)$, the hologram must have a transfer function that is proportional to $\hat{U}(u, v)$, which means an intensity transfer function proportional to $I(u, v)$ and a phase transfer function equal to $\exp[i\psi(u, v)]$. With a single hologram, the intensity transfer function can be made by absorption only. This will inevitably reduce the efficiency.

The losses that are due to absorption by the intensity transfer function are minimized if the variations of the object irradiance in the hologram plane are minimized, i.e.,

$$\iint [I(u, v) - \langle I\rangle]^2 \mathrm{d}u\mathrm{d}v \rightarrow \min. \quad (8)$$

Because we are interested only in the intensity distribution of the object the phases ϕ_m are free parameters. For determining the optimum phases, the irradiance $I(u, v)$ given by Eq. (4) is introduced into expression (8). We get

$$\iint \left[\sum_{m<n}^{N} A_m A_n \cos(\Omega_{mn})\right]^2 \mathrm{d}u\mathrm{d}v \rightarrow \min, \quad (9)$$

which means that the intermodulation terms must be minimized. The intermodulation terms can be rewritten by collecting terms of the same spatial frequency, namely

$$\sum_{m<n}^{N} A_m A_n \cos(\Omega_{mn}) = \sum_{k=1}^{N-1}\sum_{m=1}^{N-k} A_m A_{m+k} \cos(2\pi ksu + \phi_m - \phi_{m+k}) = \sum_{k=1}^{N-1} B_k \cos(2\pi ksu + \Phi_k), \quad (10)$$

where $k = m - n$. The coefficients B_k are obtained from

$$B_k{}^2 = \left[\sum_{m=1}^{N-k} A_m A_{m+k} \cos(\phi_m - \phi_{m+k})\right]^2 + \left[\sum_{m=1}^{N-k} A_m A_{m+k} \sin(\phi_m - \phi_{m+k})\right]^2. \quad (11)$$

Expression (9) then becomes

$$\iint \left[\sum_{k=1}^{N-1} B_k \cos(2\pi ksu + \Phi_k)\right]^2 \mathrm{d}u\mathrm{d}v \rightarrow \min. \quad (12)$$

Since the intermodulation terms $B_k \cos(2\pi ksu + \Phi_k)$ in expression (12) have different spatial frequencies, they are orthogonal and therefore one gets, from expression (12),

$$\sum_{k=1}^{N-1} B_k{}^2 \rightarrow \min. \quad (13)$$

Expression (13), together with Eq. (11), supplies the criterion for determining the optimum phases ϕ_m for a fan-out element with maximum efficiency.

The criterion in expression (13) reduces the intermodulation terms of Eq. (4) to a minimum but there is still a residual intermodulation. However, to avoid any absorption in the hologram plane, and also for fabrication reasons, we opt for a pure phase element. The phase is implemented as a smooth surface relief hologram without quantization. Thus the intensity transfer function of the fan-out element is clipped to $I(u, v) = 1$. The phase transfer function is equal to $\exp[i\psi(u, v)]$, as obtained for the optimum phases ϕ_m from Eqs. (2) and (3).

Clipping the residual intermodulation terms hardly alters the high efficiency, but it does reduce the uniformity of the fan-out. The amplitudes A_m' of the reconstructed spots are slightly different from the desired amplitudes A_m that are assumed for the recorded virtual light sources (Fig. 2). Furthermore, some weak side spots appear on each side of the desired N beams. There are different solutions for solving the uniformity problem. One is to add additional weak light spots to the virtual recording light sources. Thus the new parameter set contains N' ($N' > N$) light sources, where the intensity of N object beams only is of interest. Now the minimum of expression (8) can be reduced significantly. The effect of clipping becomes negligible. The readout of this fan-out produces N' light spots with perfect uniformity of the amplitudes A_m' for $m = 1$ to N. On the other hand, the $N' - N$ additional light spots (A_i, ϕ_i) increase the number of optimization parameters. As a result, the computing time rises strongly. Therefore for improving the uniformity of the fan-out, we propose another optimization process. By changing the amplitudes of the recorded virtual light sources slightly to $A_m^{(n)}$, the resulting amplitudes $A_m'^{(n)}$ in the output can be balanced; the efficiency does not decrease much.

Below we demonstrate the optimization step by step.

III. Application of the Optimization

First Optimization

For weighted fan-outs, any distribution of the A_m can be assumed and optimized by following the procedure described in Section II. However, here we treat only the particular case of uniform fan-outs ($A_m = 1$). For symmetry considerations, we impose an even distribution of the phases ($\phi_m = \phi_{N+1-m}$). In this case, Eq. (11) reduces to

$$B_k = \sum_{m=1}^{N-k} \cos(\phi_m - \phi_{m+k}). \tag{14}$$

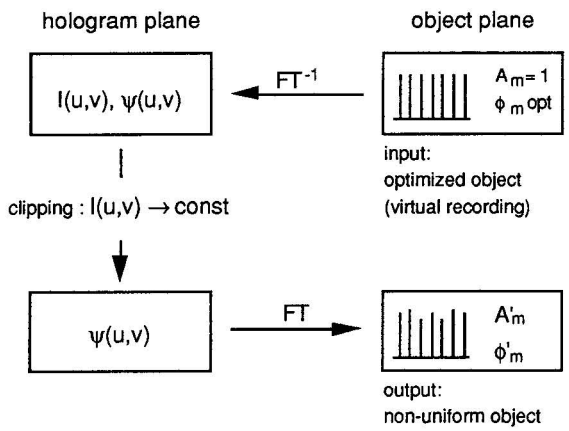

Fig. 2. First optimization process for the phases ϕ_m to gain high efficiency. The reconstructed object after clipping is nonuniform ($A_m' \neq 1$).

From expression (13) and Eq. (14) we get the optimum phases ϕ_m. The minimum in expression (13) is found by numerical optimization with the Downhill simplex method.[7] Figure 3 shows the optimization procedure, and Table I lists the optimum phases ϕ_m.

From the optimized set of phases ϕ_m, the field $\hat{U}(u, v)$ in the hologram plane and the corresponding intensity $I(u, v)$ and phase $\psi(u, v)$ are obtained through Eqs. (2) and (3). After clipping the intensity transfer function to $I(u, v) = 1$, we get a phase-only fan-out element with phase $\psi(u, v)$, which is shown in Fig. 4. We calculate the reproduced field in the object plane, which now consists of N spots with amplitudes $A_m' \neq 1$, as listed in Table I. The uniformity error is due to clipping of the residual intermodulation terms in the intensity transfer function $I(u, v)$ of the hologram (Fig. 2).

For a nine-spot fan-out element, this first optimization leads to 99.38% of the incident light being diffracted into the nine beams with ±5.35% uniformity error.

We have imposed a symmetrical distribution of phases ($\phi_m = \phi_{m+1}$). Optimization runs without this restriction have also been performed. For odd fan-out numbers, we never found higher efficiencies with nonsymmetrical phases. However, we did find higher efficiencies with nonsymmetrical phases for even fan-out numbers. Therefore the restriction of symmetrical phase has been dropped for the even fan-out numbers.

If uniformity is more important than efficiency, we continue with the second optimization step.

Second Optimization

Uniformity errors can be minimized by a second optimization procedure, which is shown in Fig. 5. We now maintain the optimum phases ϕ_m from the first optimization and change the amplitudes A_m, until perfect uniformity in the reproduced image ($A_m' = 1$) is obtained after clipping $I(u, v)$ in the hologram plane. The amplitudes $A_m^{(n)}$ of the virtual sources are changed individually at each iteration loop of the optimization process to correct for the nonuniform amplitudes $A_m'^{(n)}$ of the diffracted spots. The virtual source amplitudes $A_m^{(n+1)}$ for the next iteration are

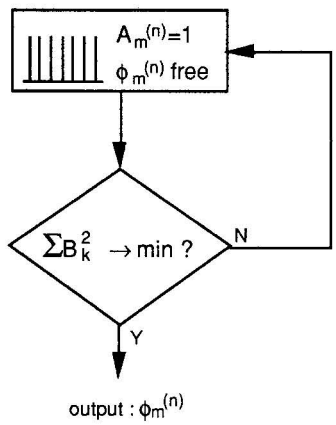

Fig. 3. Numerical optimization of phases for maximum efficiency.

Table I. Highly Efficient 9-Beam Fan-Out Element with Amplitude and Phase of the Virtual Recording Light Sources and the Resulting Light Spots

	Optimum Virtual Recording Spots		Outgoing Spots	
m	A_m	ϕ_m	A_m'	ϕ_m'
1	1	1.772	0.947	1.772
2	1	0.135	0.994	0.136
3	1	3.887	0.991	3.887
4	1	2.455	1.000	2.453
5	1	3.142	0.964	3.142
6	1	2.455	1.000	2.453
7	1	3.887	0.991	3.887
8	1	0.135	0.994	0.136
9	1	1.772	0.947	1.772

obtained from

$$A_m^{(n+1)} = A_m^{(n)} \frac{\langle A_m'^{(n)} \rangle}{A_m'^{(n)}}, \tag{15}$$

where $\langle A_m'^{(n)} \rangle$ is the average over all the diffracted amplitudes. The ratio $A_m'^{(n)}/\langle A_m'^{(n)} \rangle$ represents the weight of the mth diffracted amplitude and serves as the correction factor for the next iteration $(n + 1)$. The new optimized set of amplitudes A_m and phases ϕ_m of the virtual sources for the 9-beam fan-out element is shown in Table II.

This parameter set produces the intensity $I(u, v)$ and the phase $\psi(u, v)$ in the hologram plane. After clipping $[I(u, v) = 1]$ the reproduced spot amplitudes are perfectly uniform (see Table II). The fan-out phase distribution $\psi(u, v)^{(n)}$ is similar to that shown in Fig. 4. This second optimization has reduced the efficiency only slightly, from 99.38% to 99.28%.

IV. Discussion: Results of Numerical Optimization

We have applied our optimization methods to fan-out elements with different numbers N of beams. The computed efficiencies and uniformities resulting from the first and second optimization are shown in Table III.

For the 9-beam element, the computing time on a Micro VAX 3400 computer was ~250 ms for the efficiency optimization and ~900 ms for the uniformity optimization. The computing time for large

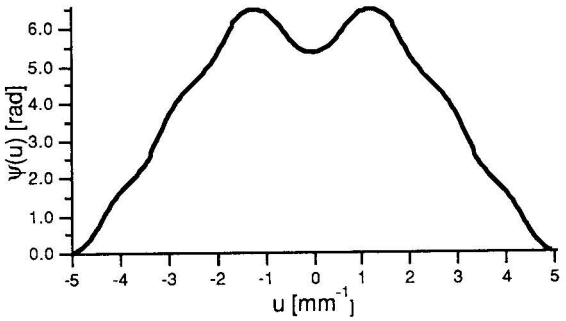

Fig. 4. Phase transfer function $\psi(u, v)$ of a high-efficiency 9-beam fan-out element.

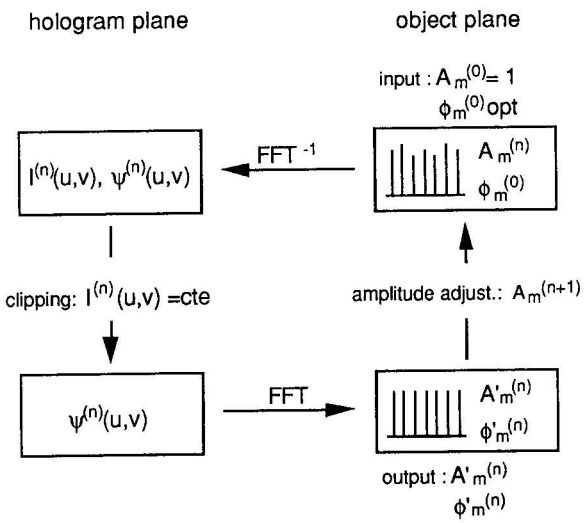

Fig. 5. Second optimization step (uniformity): $\phi_m^{(0)}$ comes from the first optimization step and (n) counts the number of iterations.

fan-outs can be reduced considerably by choosing a good starting parameter set. Good starting sets can be obtained by cascading optimum solutions of smaller fan-outs, as shown in Fig. 6. For example, an efficient 117-beam fan-out is obtained by cascading the two optimized solutions for $N = 9$ and $N = 13$.

Adding or subtracting a few points in the solution for a large optimized fan-out also gives a good starting parameter set. For example, the 100-beam fan-out has been obtained just by taking away one virtual source in the optimum solution for 101 beams.

Although the results of the optimization have been implemented only for a one-dimensional on-axis element, they can also be used for two-dimensional elements and for off-axis elements. The two-dimensional $M \times N$ parameter set is defined by $A_{ij} = A_i A_j$ and $\phi_{ij} = \phi_i + \phi_j$, where $i \in [1 \ldots M]$ and $j \in [1 \ldots N]$. For example, an optimized 9×9 fan-out element leads to 98.6% efficiency with perfect uniformity.

Reflection fan-out elements can be obtained by deposition of a reflective coating on a specially designed kinoform relief. Another solution is to replay the fan-out element under total internal reflection

Table II. Perfectly Uniform 9-Beam Fan-Out Element with Amplitude and Phase of the Virtual Recording Light Sources and the Resulting Light Spots

	Optimum Virtual Recording Spots		Outgoing Spots	
m	$A_m^{(n)}$	$\phi_m^{(n)}$	$A_m'^{(n)}$	$\phi_m'^{(n)}$
1	1.059	1.772	1.000	1.769
2	0.957	0.135	1.000	0.134
3	0.987	3.887	1.000	3.888
4	0.998	2.455	1.000	2.451
5	1.022	3.142	1.000	3.155
6	0.998	2.455	1.000	2.451
7	0.987	3.887	1.000	3.888
8	0.957	0.135	1.000	0.134
9	1.059	1.772	1.000	1.779

Table III. Efficiency and Uniformity Issued From First and Second Optimizations

	Efficiency Optimization		Uniformity Optimization	
N	η (%)	ΔI_m (%)	η (%)	ΔI_m (%)
3	94.9	±23.0	92.6	<0.1
5	98.0	±28.2	92.1	<0.1
7	98.0	±22.3	96.8	<0.1
9	99.4	±5.4	99.3	<0.1
10	98.2	±30.6	95.4	<0.1
11	98.8	±21.6	97.7	<0.1
13	99.3	±27.3	96.3	<0.1
21	99.2	±16.9	98.6	<0.1
81	99.3	±20.7	97.0	<0.1
100	98.8	±32.7	97.4	<0.1
101	99.1	±26.8	98.0	<0.1
117	99.2	±43.4	97.6	<0.1

conditions. Such elements do not need special reflective coatings and are of great interest for integrated planar optics. Two-dimensional and total internal reflection fan-out elements are actually under investigation.

Another interesting type of element combines fan-out and focusing properties. Focusing can be added by a Fresnel lens superposed to the fan-out phase structure, the whole structure being written in one raster scan.

The photoresist relief structure of all elements discussed above can be converted into a metal master relief by electroplating techniques for mass production of low-cost replicas.

V. Comparison with Other Optimization Procedures

The first and second optimization steps described Section III are quick. They lead to fan-out elements with good efficiency and perfect uniformity. Some other optimization procedures have also been tested for comparison.

Amplitude Optimization

In the described first optimization step we minimize the variance of the object irradiance in the hologram plane (expression 8). Wyrowski defines an upper limit for the diffraction efficiency of phase-only holograms [Eq. (19b) of Ref. 8]. This upper limit is reached when the variations of the object field amplitude $|\hat{U}|$ around its average value $\langle|\hat{U}|\rangle$ are minimum. This leads to a different optimization criterion, namely,

$$\iint (|\hat{U}| - \langle|\hat{U}|\rangle)^2 \mathrm{d}u\mathrm{d}v \rightarrow \min. \tag{16}$$

We have optimized a few fan-outs by following this criterion. The optimization process was much slower. It yields the same set of optimum phases.

Phase Spectrum Optimization

In this optimization we work with a set of parameters that are defined in the hologram plane. The grating phase function is constructed from a limited sum of harmonics:

$$\hat{U}(u, v) = \exp[i\psi(u, v)], \tag{17}$$

$$\psi(u, v) = \sum_{p=1}^{P} A_p \cos(2\pi p u). \tag{18}$$

The amplitudes A_p of these harmonics are the optimization parameters, while the efficiency and the uniformity in the object plane are the criteria for the optimization. Again, this optimization process is much slower. For a 5-beam fan-out element, built with the 10 first odd harmonics, 3 min of computing time on a MicroVAX 3400 was necessary to find the same optimum phase function with 92.1% efficiency and <0.1% uniformity error, as was already shown in Table III. However, this method is more general and can easily take into account the limitations for the resolution of the hologram writing system by limiting the number of harmonics.

VI. Kinoform Fabrication

The above results can be used for the fabrication of either an on-axis or an off-axis hologram (recorded with a reference beam). For our application we have opted for an on-axis hologram in which the phase function is transferred into photoresist as a surface relief element. By the time of fabrication of the kinoform, only the first optimization step had been developed. Therefore only the phase $\psi(u, v)$, which results from the first optimization, has been implemented.

The element was fabricated at the Paul Scherrer Institute, Zürich, where a high precision laser-beam writing system is available.[4] A photoresist layer is deposited on a flat substrate. It is exposed with a

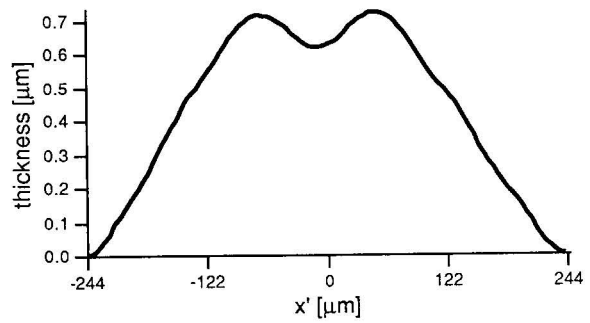

Fig. 6. Cascading parameter sets.

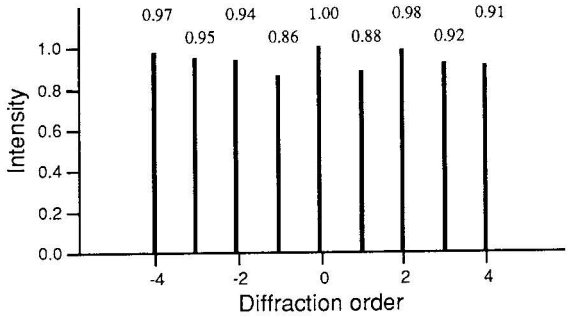

Fig. 7. Profile thickness of the fabricated fan-out.

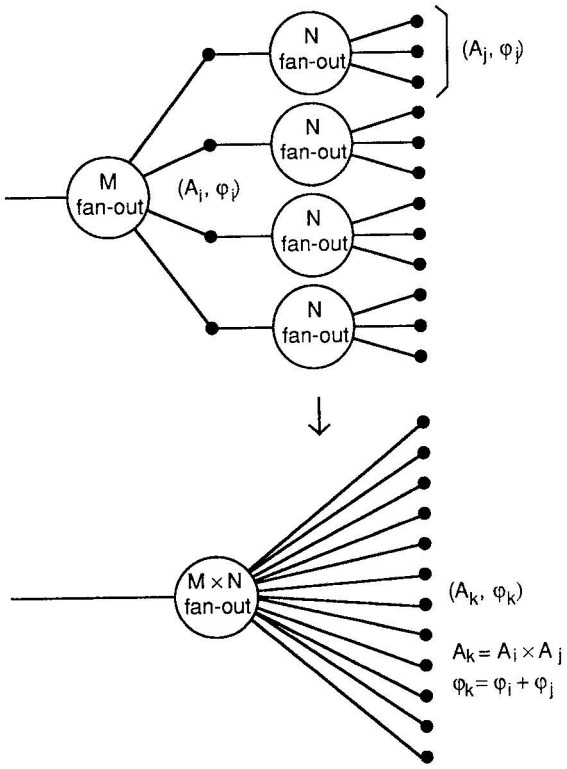

Fig. 8. Relative intensities of the fabricated fan-out.

scanning laser beam of controllable intensity. Then it is etched in developer. The etching rate depends on the received exposure dose. The fidelity of the relief phase element relies on the knowledge and reproducibility of the photoresist response. Finally the phase element is baked and measured with a stylus profilometer. One typical measured profile of photoresist thickness is shown in Fig. 7.

The element has been tested by analyzing the Fourier image that is produced when illuminated with a plane-wave laser beam (Fig. 1). The diffracted beams are focused onto a CCD camera with a lens of 100-mm focal length. The measured relative values of the spot intensities are shown in Fig. 8. The uniformity is within ±7%. The absorption of the substrate and the photoresist has been measured to be 2%. The measured efficiency, i.e., the fraction of the transmitted light that was focused into the nine spots, was 92%.

VII. Conclusions

A two-step method of optimizing the transfer function of fan-out elements has been developed. The first step optimizes the efficiency. The result is an element with minimized variations of the intensity transfer function. To obtain a pure phase element, the residual intermodulations in the intensity transfer function are clipped. This introduces uniformity errors. The second step optimizes the uniformity of the pure phase element. The efficiency is only slightly reduced. The theoretical efficiency for a perfectly uniform nine-beam fan-out is better than 99%.

Both optimization steps are fast compared with other methods. The computing time for a 9-beam element is ~250 ms for the first step and 900 ms for the second step on a MicroVAX 3400. Our optimization parameters are defined in the object plane. Generally, optimization in the hologram plane requires more parameters and, consequently, more computing power.

The optimization method is easily extendable to large and to two-dimensional fan-outs. Good starting parameters and, therefore, a short computing time for large fan-outs are obtained by cascading optimum solutions of smaller fan-outs. The optimum solution for a 117-beam fan-out with a 97.6% efficiency and a less than 0.1% uniformity error has been obtained from cascading the two optimized solutions for a nine-beam and a 13-beam fan-out.

We have recorded an optimized 9-beam fan-out as a surface relief kinoform with a laser-beam writing system. The implemented phase is a result of the first optimization step and has a theoretical efficiency of 99.38% and a uniformity of ±5.35%. This element has been investigated experimentally. It shows a high efficiency (92%) and a moderate uniformity (±7%), which is due mainly to fabrication tolerances.

References

1. J. N. Mait, "Design of binary-phase and multiphase Fourier gratings for array generation," J. Opt. Soc. Am. A **7,** 1514–1528 (1990).
2. J. Turunen, J. Fagerholm, A. Vasara, and M. R. Taghizadeh, "Detour-phase kinoform interconnects: the concept and fabrication considerations," J. Opt. Soc. Am. A **7,** 1202–1208 (1990).
3. M. T. Gale, G. K. Lang, J. M. Raynor, and H. Schütz, "Fabrication of micro-optical components by laser writing in photoresist," in *Micro-Optics* II, A. M. Scheggi, ed., Proc. Soc. Photo-Opt. Instrum. Eng. **1506,** 65–70 (1991).
4. M. T. Gale, G. K. Lang, J. M. Raynor, and H. Schütz, "Fabrication of kinoform structures for optical computing," Appl. Opt. **31,** 5712–5715 (1992).
5. H. P. Herzig, R. Dändliker, and J. M. Teijido, "Beam shaping for high power laser diode arrays by holographic optical elements," in *Holographic Systems, Components and Applications,* Conference Publ. 311 (Institution of Electrical Engineers, London, 1989), pp. 133–137.
6. H. P. Herzig, D. Prongué, and R. Dändliker, "Design and fabrication of highly efficient fan-out element," Jpn. J. Appl. Phys. **27,** L1307–L1309 (1990).
7. W. H. Press, B. P. Flannery, S. A. Teukolsky, and W. T. Vetterling, *Numerical Recipes in Pascal* (Cambridge U. Press, Cambridge, 1989)
8. F. Wyrowski, "Diffractive optical elements: iterative calculation of quantized, blazed phase structures," J. Opt. Soc. Am. A **7,** 961–969 (1990).